

Measuring Seismometer Nonlinearity on a Shake Table

by Erhard Wielandt and Mark Zumberge

Abstract We have measured the nonlinear distortion in six broadband seismometers on the vertical shake table at the Institute of Geophysics and Planetary Physics La Jolla: a vertical STS1, three STS2s, a CMG-3T, and a Trillium 240. In each case, low-frequency intermodulation of a two-tone signal was observed for six frequency pairs near 0.25, 0.5, 1, 2, 4, and 8 Hz at a beat frequency of 0.02 Hz. The peak velocity amplitude was 6.3 mm/s, which is about half of the operating range of an STS2 or CMG-3T. We found similar distortion levels in all seismometers: The average over all distortion ratios is $-96 \text{ dB} \pm 7 \text{ dB}$ (std. dev.) in terms of equivalent ground acceleration, with a tendency to higher distortion at higher frequencies. When the same signals are expressed as electric output voltages or equivalent ground velocities, ratios are much higher and increase rapidly with frequency: around -65 dB at 1 Hz and around -40 dB at 8 Hz. The distortion of seismic signals cannot be predicted from the distortion of electrical signals fed into the calibration coil, and the electrical distortion is about 30 dB lower in one of the STS2s. Low-frequency distortion of the table motion has a level of -140 dB at 1 Hz in terms of acceleration, which is far below that of all seismometers. This number does not indicate a super-linear table motion but results from expressing the distortion present in the table displacement at -72 dB as a ratio of accelerations. What may seem to be a trivial conversion has a very practical implication: The linearity of seismometers can be tested on moderately performing shake tables.

Basics

Nearly all modern broadband seismometers operate on the same principle: The displacement of a proof mass that is mounted on a spring or a pendulum is monitored electronically. A force, either electrostatic or magnetic, is imposed on the proof mass to keep its position constant. The magnitude of the feedback force is proportional to the ground acceleration. Usually the feedback signal is processed with analog electronics to provide an output voltage from the seismometer proportional to ground velocity. One desires a linear relationship between ground velocity and the output voltage with a gain that is constant over a broad range of frequency. Most seismometers contain a calibration coil, which is a separate device that can be used to impart an additional force on the proof mass to calibrate the seismometer and all of its control electronics.

Nonlinear distortion in seismometers has traditionally, if at all, been measured by injecting a two-tone signal into the calibration coil and observing low-frequency intermodulation at the output (Peterson *et al.*, 1980; Hutt *et al.*, 2009). A two-tone signal is a test signal consisting of two sinusoids very close in frequency, while the intermodulation signal is the one at a frequency of the difference between the two-tone signals and has an amplitude that would be zero if the system were linear. Such an experiment does not duplicate, however,

the internal forces resulting from an equivalent seismic input. The calibration coil is normally part of the same force transducer that is used for feedback; some sensors do not even have separate coils and simply add the calibration current to the feedback current. Any reasonable feedback circuit of the force–balance type will then nearly compensate the calibration current with a feedback current of opposite polarity. So only a small fraction of the calibration current is converted into a force. The acceleration of the pendulum relative to an inertial reference remains small, and inertial forces acting on structural components such as hinges are likewise small. On the other hand, in the presence of a seismic signal, the pendulum moves with the frame, the force transducer must provide a much larger force to accelerate it, and forces in the hinges are also larger. Furthermore, cross-axis accelerations are present, which cannot be simulated electrically. The linearity of seismic sensors therefore cannot be tested thoroughly with an electric input into the calibration coil.

Shake tables with a precision adequate to measure distortion in seismometers are rarely available to seismological institutions. Besides, many seismologists are discouraged by the belief that for such an experiment the table must have a better linearity than the seismometer, which would be a very restrictive specification (linear, in this context, means the

table's position is proportional to an electronic control signal). The following considerations show that this concern is unfounded.

- 1 It does not matter how accurately the table follows its control signal or how distortion free that signal is. What matters is how well we know the motion. If we can measure and record it with sufficient precision, then we can predict the linear response of the seismometer, subtract it from the actual one, and retain only the nonlinear distortion originating in the seismometer.
- 2 When the input signal of a linear system is periodic and its average over one period equals zero, then the same is true for the output signal. When the servo system of a shake table is nonlinear, the mean position of the table may be offset from zero but not its mean velocity or acceleration—the table cannot run away. In response to a two-tone input, the average table position varies with the envelope of the control signal. This results in a spurious displacement signal at the beat frequency whose amplitude does not depend, however, on that frequency (we give a mathematical formulation in the next section.) The amplitudes of the associated velocity and acceleration signals are then proportional to the first and second power of the beat frequency, respectively, so they become smaller at lower beat frequencies. On the other hand, low-frequency intermodulation in a seismometer does not disappear at low beat frequencies; a sinusoidal signal of constant amplitude (equivalent to a two-tone signal with an infinite beat period) will cause a constant offset in the apparent ground acceleration when, for example, the transducer for the feedback force is nonlinear. In a two-tone test one can thus always make the low-frequency component of shake-table distortion negligible compared to that of the seismometer by using a sufficiently low beat frequency. A practical limitation may result from instrumental, seismic, and environmental low-frequency noise, but not from nonlinearity in the shake table. In our experiments we did not see such a limit, and because the intermodulation signal is monochromatic, it can theoretically always be extracted given enough time. In a preliminary test, we got the same result (in terms of acceleration) for beat frequencies of 0.02 and 0.01 Hz.

We thus have two methods at our disposal to reduce the expression of shake-table nonlinearity in the output signal of the seismometer. While their combination is especially powerful, in most cases we found that low-frequency acceleration distortion from the table at a beat frequency of 0.02 Hz is negligible and removing it by linear modeling only confirms this. Only at our lowest signal frequency of 0.25 Hz were contributions from the table and from the seismometer of comparable magnitude so that the former had to be removed by linear modeling.

While these considerations seem to be independent of the orientation of the sensor, an additional difficulty exists for horizontal sensors: In the presence of gravity they are sensitive

to tilt. Undesired tilt of shake tables is already noticeable in ordinary calibration experiments. Nonlinear distortion in the table motion or in its mechanical coupling with tilt is then seen as an apparent acceleration. It no longer disappears in the low-frequency limit, and in order to model it, we must be able to measure a small nonlinear component in the already small tilt of the table. Our ability to do so is certainly very limited. We expect, however, that distortions in all output signals from a Galperin type (homogeneous–triaxial) sensor are similar.

A Simple Model of Seismometer Nonlinearity

Of the many possible forms and causes of seismometer nonlinearity, we will mathematically formulate only the simplest case for which a supposedly constant mechanical or electrical property, such as spring stiffness, transducer responsivity, or electronic gain, in reality depends on the instantaneous input. More specifically, we would like a sensor or transducer to be governed by $s_{\text{out}} = c \times s_{\text{in}}$ for which s_{out} is the output signal, s_{in} is the input signal, and c is constant, but in fact there may be a term proportional to s_{in}^2 (or stated another way, c is not constant but depends slightly on s_{in}). The electromagnetic force transducer (a voice coil) is an obvious example of this behaviour. When a current flows through the coil in a constant magnetic field, it experiences a force that is proportional to the current. But the field is not constant; the coil induces an additional magnetization in the permanent magnet and its pole pieces. This gives rise to a quadratic term in the relationship between current and force. Also, neither the field nor the wire windings are perfectly homogeneous, so the responsivity depends on the position of the coil and thus on the seismic signal. In a feedback loop, in general the coil does not move in phase with its current, and the relationship becomes noninstantaneous and frequency dependent. Eddy currents in the pole pieces of the magnet may cause a noticeable force opposite to the quadratic magnetic attraction at high frequencies. All these effects result in an amplitude modulation of the signal by itself or of one component of the signal by another, hence the term “intermodulation”. There are several other potential sources of nonlinearity in a seismometer, some of which will be considered later.

In the simplest case of an instantaneous quadratic nonlinearity, we should be able to describe signal distortion by the general relationship

$$Z(t) = g[z(t) + (1/a_0)z(t)^2] \quad (1)$$

between the instantaneous input $z(t)$ (ground velocity, for example, or feedback current) into the nonlinear device and the instantaneous output $Z(t)$ (seismometer output voltage, for example, or feedback force), such that g is a constant gain factor or responsivity and a_0 controls the nonlinearity. In order to determine the magnitude of the quadratic term, we apply a two-tone signal: $z(t) = a(\cos \omega_1 t + \cos \omega_2 t)$ with $\omega_1 \approx \omega_2$. The output signal is then

$$\begin{aligned}
Z(t) &= g[a(\cos \omega_1 t + \cos \omega_2 t) \\
&\quad + (1/a_0)a^2(\cos \omega_1 t + \cos \omega_2 t)^2] \\
&= ga(\cos \omega_1 t + \cos \omega_2 t) \\
&\quad + \frac{ga^2}{2a_0}[\cos 2\omega_1 t + \cos 2\omega_2 t + 2 \cos(\omega_1 + \omega_2)t] \\
&\quad + \frac{ga^2}{a_0}[1 + \cos(\omega_1 - \omega_2)t]. \tag{2}
\end{aligned}$$

In addition to the terms that are linear in the signal amplitude and have the frequencies ω_1 and ω_2 , we now find five terms with frequencies that were not present in the input signal. Three of the terms oscillate twice as fast as the input signal: $2\omega_1$, $2\omega_2$, and $\omega_1 + \omega_2$. One of the terms oscillates slowly with the difference (beat) frequency $\omega_1 - \omega_2$, and one of the terms is static. The term with $\omega_1 - \omega_2$, which can be isolated experimentally with a band-pass filter, has an rms amplitude of $\sigma_{\text{beat}} = (\sqrt{2}/2)ga^2/a_0$ independent of the test and beat frequencies. (We now see that a_0 in equation 1 is the hypothetical input amplitude for which the distortion at the beat frequency has half of the power of the linear signal.) The rms amplitude of the linear two-tone signal is $\sigma_{\text{two-tone}} = ga$. The quantity $D = \sigma_{\text{beat}}/\sigma_{\text{two-tone}}$ is what we call the distortion ratio, and it is proportional to the signal amplitude a . Once the distortion ratio D has been measured with a two-tone test signal of peak amplitude $2a$, the coefficient for the quadratic intermodulation ($1/a_0$) in equation (1) can easily be calculated: $1/a_0 = \sqrt{2}D/a$.

Although the distortion ratio quantifies only one out of five nonlinear terms, according to equation (2) the other terms have similar amplitudes when the quadratic model is applicable. Even if it is not, we normally do not care much about them. Moderate high-frequency distortion can be tolerated in most cases because the complexity of seismic waveforms prevents the interpretation of signals down to that amplitude level. Low-frequency intermodulation, on the other hand, interferes with the reconstruction of ground displacement because this process involves at least one integration (generally, three) and can drastically amplify low-frequency components of the signal. We will give a numerical example in the [Appendix](#).

We do not see a straightforward way to measure high-frequency distortions (harmonics) of the two-tone signal in our broadband seismometers because of the difficulty of separating them from those of the table. The frequency ratio between distortion and signal works against us, and we find it difficult to model the seismometer output accurately from the table motion, probably because the motion is not sufficiently uniform at high frequencies to be picked up at the edge of the platform as we did. Some theoretical properties of quadratic and higher-order distortion are discussed in the [Appendix](#).

In our mathematical model the distortion ratio does not depend on the test frequencies. Seismometers are not so simple. Internal electrical signal levels, and therefore distortion levels, depend on the frequencies of the test signal, and a

given distortion of an electric signal corresponds to different ratios of equivalent ground displacement, velocity, and acceleration (a numerical example is given in [Hutt et al. \[2009\]](#)). We must also distinguish between electrical and mechanical input. The distortion ratio of a seismometer is not a single, clearly defined number. An undetailed specification such as “Nonlinearity ___dB” as may be found in some seismometer data sheets makes no sense to us.

The Shake Table

The shake tables at the Institute of Geophysics and Planetary Physics (IGPP) (one vertical and one horizontal) were obtained from the former Soviet Union in 1990, as part of the cooperative Eurasian Seismic Studies Program. (Another set of slightly smaller tables was later installed at the Albuquerque Seismological Lab.) The platform of each table, 51 by 51 cm, is guided by levers in a parallelogram geometry so that it can move by ± 20 mm on a circular arc of a 70 cm radius; the joints are robust crossed flexural hinges. The tables are driven by large voice coils. Internal mechanical resonances limit their usefulness for distortion tests to frequencies well below 25 Hz. Table motion was originally sensed by a capacitive displacement transducer and controlled by a custom-made electronic feedback circuit. These were later replaced by modern components (an LVDT, a PID servo circuit, and an audio power amplifier). For the present experiments we temporarily added an interferometric displacement transducer of the same general design as used in an optical seismometer ([Zumberge et al., 2010](#)). Its precision is so high (-130 dB linearity with 0.2 nm resolution) that its digital output signal can be considered to represent the table motion exactly (although only at one edge of the table where the cube-corner reflector is attached). The usefulness of the shake table for seismometer testing does not depend on the precision of this transducer; a good LVDT would suffice. For the experiments described herein, we used only the vertical shake table, which is shown in [Figure 1a,b](#).

Experimental Procedure

We excited the vertical shake table with a two-tone signal ([Fig. 2](#)) from a two-channel, digital sinewave generator whose signals, of equal amplitude, were combined over a passive, first-order high-pass filter ([Fig. 3](#)) whose purpose was to suppress intermodulation and low-frequency noise from the generators. We recorded the table displacement with a digital Michelson interferometer and the seismometer output with a Quanterra Q330HR. Mechanical peak amplitudes of the two-tone signal were:

- 4 mm at 0.25 and 0.27 Hz
- 2 mm at 0.50 and 0.52 Hz
- 1 mm at 1.00 and 1.02 Hz
- 0.5 mm at 2.00 and 2.02 Hz
- 0.25 mm at 4.00 and 4.02 Hz
- 0.125 mm at 8.00 and 8.02 Hz

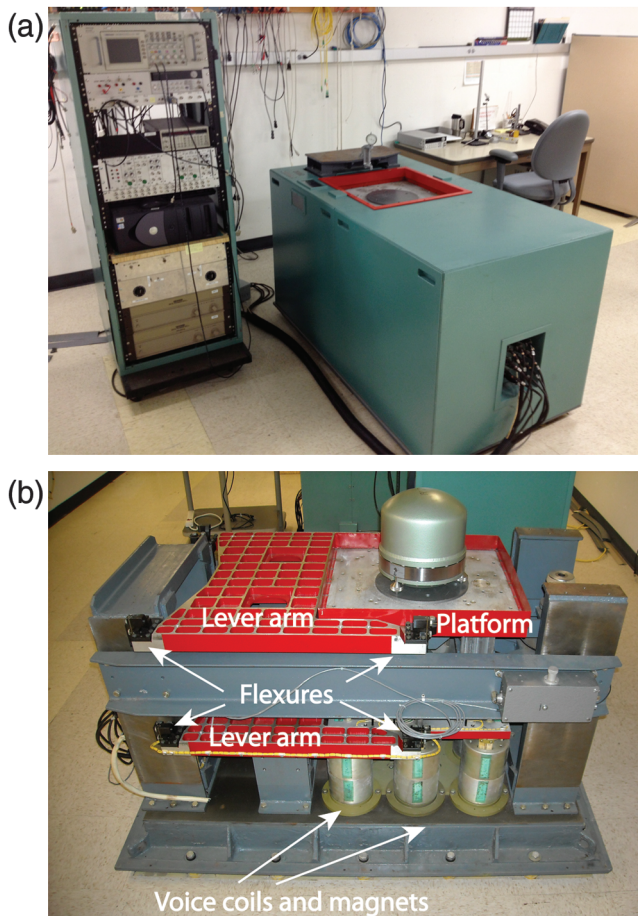


Figure 1. (a) The vertical shake table. (b) The vertical shake table with the covers removed and the interior revealed with an STS2 seismometer under test.

All these combinations result in a peak velocity of approximately 6.3 mm/s, which is close to half of the nominal operating range of the STS2 and CMG-3T seismometers and about 0.4 of the nominal range of the Trillium 240. The STS1, which has a range of 8.3 mm/s, was tested at a peak of 4 mm/s. For the graphic representation of the results, all values were normalized to a peak table velocity of 6.3 mm/s

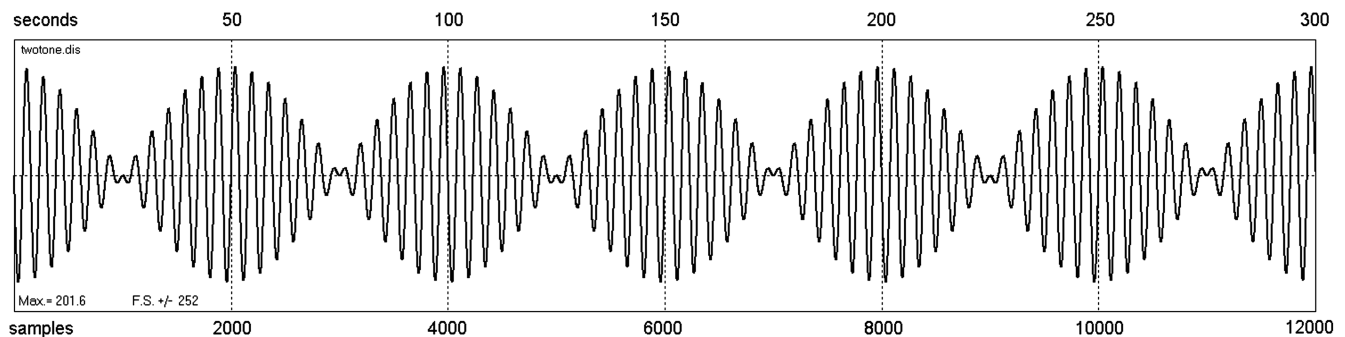


Figure 2. The synthetic two-tone signal at 0.25 and 0.27 Hz, on which Figure A1 of the [Appendix](#) is based. The circuit of Figure 3 produces the same waveform when the generators are set accordingly. The position of the table follows this control signal with an amplitude of ± 4 mm. At higher frequencies, we reduce the amplitude so that the peak velocity remains the same.

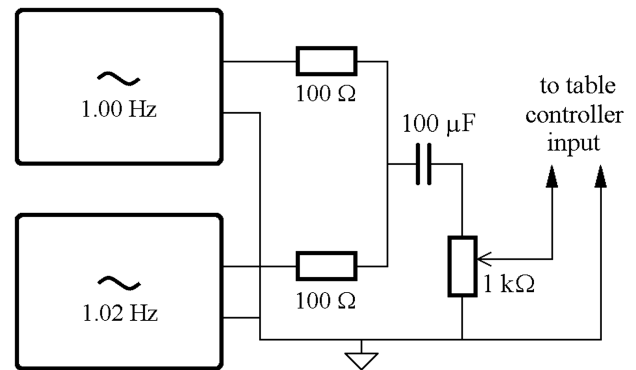


Figure 3. The circuit used to sum the outputs of two signal generators (each having 50Ω output impedance). Its purpose is to reduce low-frequency intermodulation in the control signal. The $100 \mu\text{F}$ capacitor and the $1 \text{ k}\Omega$ potentiometer form a high-pass filter with a corner frequency of 1.6 Hz, and for the 0.25 Hz signal we used $220 \mu\text{F}$. The capacitance was realized as a bank of solid-dielectric capacitors. The potentiometer serves to smoothly remove the signal from the shake-table driver, as sudden changes in the control voltage could damage a seismometer under test. A larger value for the potentiometer would allow one to use fewer capacitors; our selections were based partly on expedience.

assuming a quadratic nonlinearity and thus a distortion ratio proportional to the signal amplitude. We did not vary the beat frequency of 0.02 Hz because preliminary tests had indicated that the distortion ratio for accelerations does not depend on it.

The evaluation consisted of the following steps, entirely in the time domain: predicting the seismometer response to the recorded table displacement with a linear algorithm, subtracting the synthetic output signal from the recorded one, band-pass filtering the residual, plotting and inspecting the signals, and finally evaluating the rms amplitudes of the two-tone signal at the seismometer output and of the low-frequency intermodulation signal in the residual. For broadband-velocity sensors, the ratio of these rms amplitudes is the velocity distortion ratio, as long as the test frequencies are within the flat region of the seismometer's response curve.

Modeling the seismometer output in the time domain is not trivial because the commonly used infinite impulse

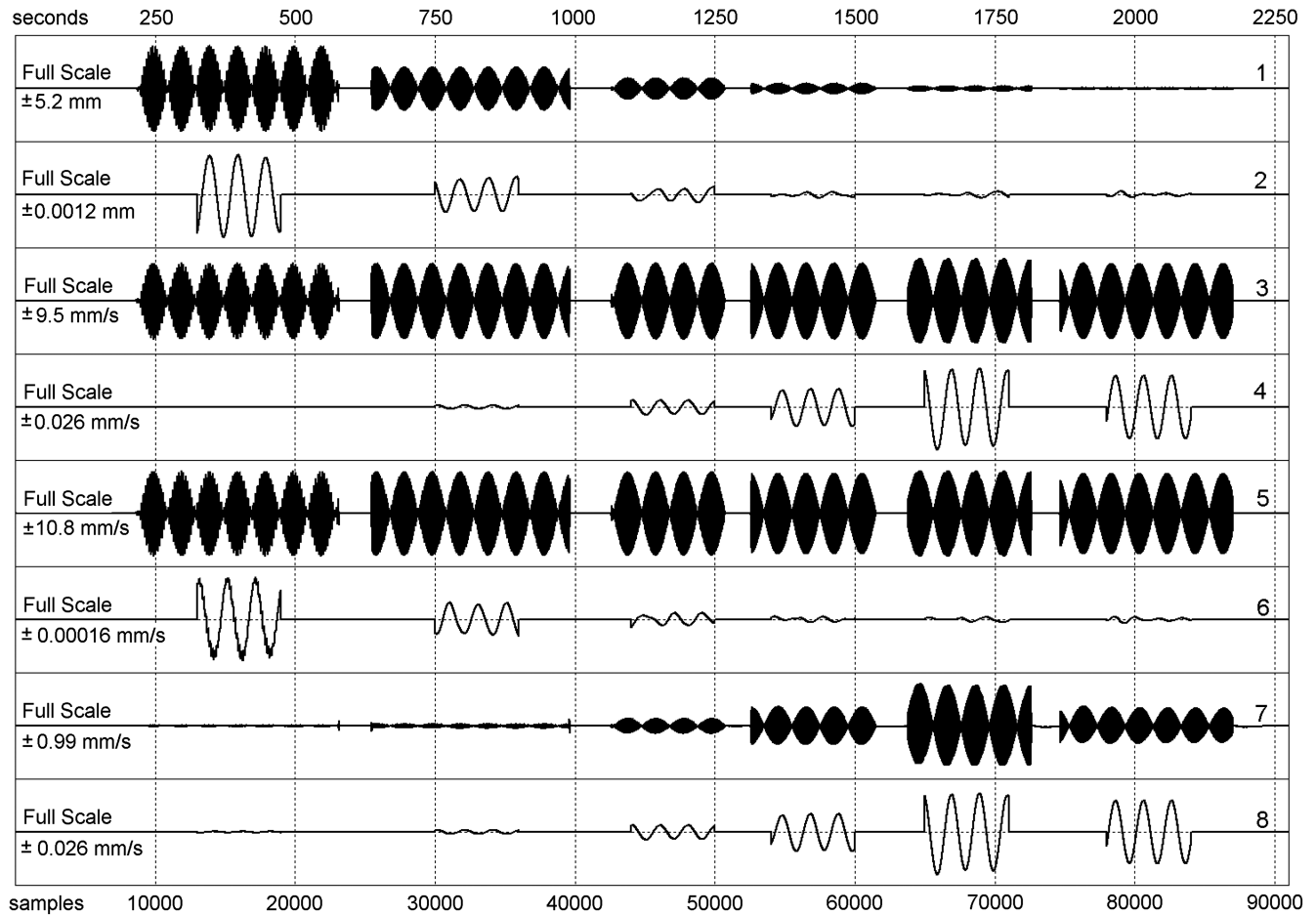


Figure 4. Modeling and filtering of the output signal. The traces are: 1—table displacement, interferometric; 3—seismometer output, equivalent to ground velocity; 5—seismometer output predicted from trace 1; 7—residual (trace 3 minus trace 5); 2, 4, 6, and 8 are the same as traces 1, 3, 5, and 7 after band-pass filtration 13.3–30 mHz (33.3–75 s). Distortions from the table cancel in the residual. Peak amplitudes of each trace are 80% of full scale.

response filters designed with the bilinear approximation cannot represent an analog system accurately. We used the CALEX software (Wielandt, 2012; see [Data and Resources](#)) that employs an impulse-invariant variety of infinite impulse response filters (Schuessler, 1981). This method is not exact either but can be made accurate enough for all practical purposes. The present version of the CALEX models the impulse response of a seismometer to within 1 ppm when the bandwidth is limited to one-quarter of the sampling frequency. In modeling the output signal, we used nominal or previously determined actual parameters for the frequency response of the seismometer but fitted a gain factor and a millisecond delay to account for gain and timing errors between the separate data acquisition systems. The experimental procedure is best explained with Figure 4.

We first explain the unfiltered traces. Six two-tone signals were successively applied (trace 1), starting with the lowest frequency of 0.25/0.27 Hz. Amplitudes were chosen so that the peak velocities were nearly the same in all cases, as is apparent from the uniform amplitudes in the velocity-proportional seismometer output (trace 3). The simulated

output signal (trace 5) is visually identical to the actual one. The misfit (trace 7) is largest at high frequencies, most likely because we did not bother to model the seismometer and digitizer responses precisely (traces 1 and 3 were recorded with technically different systems). There might also be a problem with nonuniform table motion at high frequencies. Intermodulation is not visible in the unfiltered residual.

The filtered traces (2, 4, 6, and 8) originally have switching transients at the beginning and end of the wave groups; these were blanked out in the plot for clarity. The intermodulation signal at 0.02 Hz is now clearly visible. In the table displacement (trace 2), it is largest at the lowest test frequency where the mechanical amplitude is largest. In the seismometer output (trace 4), it is large at high test frequencies where the acceleration is high, although in this case it assumes its largest value at 4 Hz. The simulated seismometer output (trace 6) contains distortion from the table only because the simulation algorithm is linear. By subtracting trace 6 from trace 4, we retain only the distortion from the seismometer (trace 8). Distortion in the Q330 digitizer is negligible in this context.

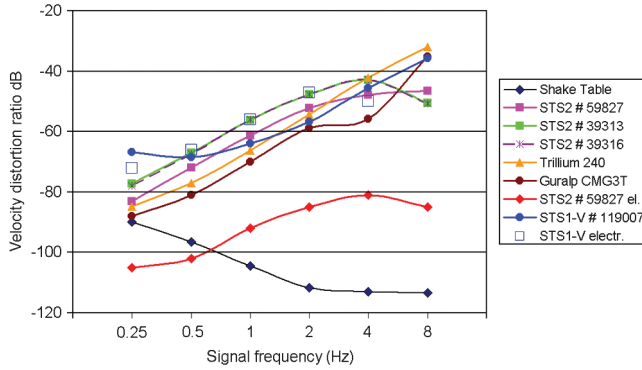


Figure 5. Seismic distortion levels in terms of equivalent ground velocity. For comparison, the electrical distortions from an STS1 and an STS2 seismometer, measured as described in the [Appendix](#), are also plotted.

To obtain the distortion ratios, we extracted segments from traces 3 and 8 corresponding to the six individual test frequencies. We computed the distortion ratio $D = \sigma_{\text{beat}} / \sigma_{\text{two-tone}}$ in decibels using $20 \times \log[(\text{trace 8 rms amplitude}) / (\text{trace 3 rms amplitude})]$ with one slight modification: D is a dimensionless number that depends on the amplitude of the input signal (a in equation 2); however, the shake-table velocity varied slightly from the nominal 6.3 mm/s peak value from test to test. To normalize the computed distortion ratios to a common velocity, we multiplied D in each case by the factor $6.3/(\text{actual peak velocity in mm/s})$.

Results

Our results are summarized in Figure 5 in terms of equivalent ground velocity and in Figure 6 in terms of equivalent ground acceleration (from $D_{\text{accel}} = D_{\text{vel}}(\omega_1 - \omega_2)/\omega_2$). The electrical distortion level of STS2 # 59827 is shown for comparison, and we describe in the [Appendix](#) how it was measured.

The figures show that the distortion ratios of the six tested seismometers are fairly uniform. Overall, ratios increase roughly with the square root of the test frequency in terms of acceleration and with power 1.5 of the test frequency in terms of velocity. Individual instruments show, however, different trends. In the following we refer to the acceleration ratios (Fig. 6). The Trillium 240 has distortion ratios nearly proportional to frequency. This is what one would expect from the simple physical model of seismometer nonlinearity formulated above because our test accelerations were proportional to the test frequency. In fact, all seismometers except the STS1-V show the expected trend between 0.5 and 2 Hz. Distortion in the STS1-V has no clear trend versus frequency, which is more difficult to explain. At higher and lower frequencies, observed ratios suggest a superposition of different frequency-dependent effects, including partial cancellation. The STS2s # 39313 and # 39316, which are two instruments from the same production batch, agree closely. Both are old instruments made in 1993

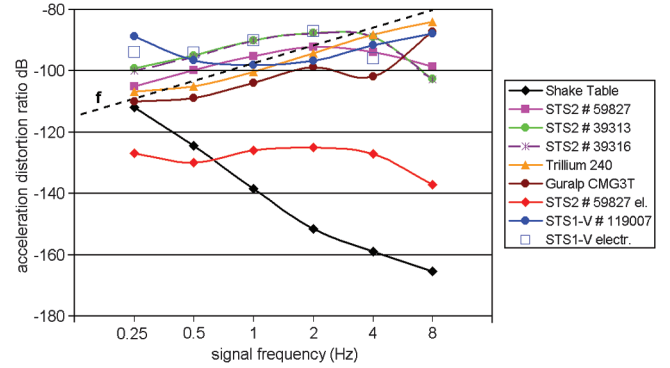


Figure 6. The same distortion levels in terms of equivalent ground acceleration. The dashed line f marks a distortion ratio that is proportional to the signal frequency, as it would result from a quadratic nonlinearity of the transducer force.

and had just returned from a factory repair when we tested them. The two lower curves represent the electrical distortion ratio of STS2 # 59827 (red), which was about 30 dB lower than on the shake table, and the distortion ratio of the shake table (black) reaching -165 dB at 8 Hz.

The electrical distortion ratio of the STS1, which was also measured, is indicated by unconnected open squares. It is comparatively large—of the same order as the distortion ratio for seismic input. This is not, however, typical for broadband seismometers. The two force transducers in the STS1 have open pot magnets and are therefore slightly non-linear but are mounted in opposite orientation. With respect to the feedback force this cancels the nonlinearity but not for the calibration input because only one of the transducers incorporates a calibration coil; the corresponding coil on the other transducer is used for integral feedback. So even if the distortions of electrical and mechanical input signals happen to be of similar magnitude, they are not related to each other. We also noted on this occasion that the hand-operated switch in the original feedback electronics that connects the calibration coil directly to the remote calibration input is unreliable and can distort the calibration current.

Possible Origins of Seismometer Nonlinearity

We have already mentioned the inherent quadratic nonlinearity of voice-coil type force transducers as a possible source of seismometer nonlinearity. The mechanical suspension of the seismic mass is not perfectly linear either. Although a few designs, such as the one used in LaCoste gravimeters or the one in Streckeisen seismometers, are known for which the quadratic term in the force vs. displacement relationship of the pendulum is theoretically zero, not all manufacturers use such a suspension because negative force feedback makes it possible to keep the mechanical displacement so small that nonlinearity of the suspension is not a limiting factor. Even in a theoretically linear suspension, tolerances of manufacture or rough handling may alter the geometry, and the effective axis of rotation may depend on forces acting on the elastic hinges

(especially if these have been damaged). Finally, a capacitive displacement transducer is not perfectly linear due to the circular motion of the capacitor plate, inhomogeneous fringe fields, and less-than-ideal performance of the electronic circuit (see, for example, Valliant *et al.*, 1986). Sensors with a geometrically linear motion of the mass may avoid some of these problems but have others.

To our knowledge, the magnitude of different nonlinear effects has never been measured separately in a broadband seismometer. This would be difficult. It is possible, however, to model the expected effects analytically if one makes plausible assumptions on the nonlinearity of individual components. We find that nonlinearity of the force transducer is most critical. Even a well-designed force transducer can limit the overall linearity of a feedback seismometer. A quadratic component of 0.01% in the feedback force is sufficient to explain an observed distortion level of an STS2 seismometers at 1 Hz. Effects from a nonlinearity in the restoring force of the spring and from the displacement transducer should typically be one or two orders of magnitude smaller.

Experimental evidence supports this prediction. As was already mentioned, we found that distortion in the STS2 is much higher for seismic input than for electrical input applied through its calibration coil. Electronic components and the displacement transducer see the same signal in both situations, so they cannot be responsible for the difference. The elongation of the spring is also the same. Distortion of seismic signals in the STS2 must mainly occur where the forces are different and where they can induce a nonlinear effect. The main suspects are therefore the force transducer and compliant parts such as the hinges and the spring whose deformation by inertial forces changes the geometry of the suspension.

A simple quadratic nonlinearity alone, however, does not completely explain our observations. Effects with a more complicated dependence on the signal amplitude, frequency, or waveform must be present. In that case the distortion ratio cannot simply be scaled to smaller signal amplitudes. Unfortunately, we did not investigate the dependence of the distortion ratios on amplitude at constant frequency. Such measurements combined with a circuit simulation might allow a better identification of nonlinear mechanisms.

Besides nonlinearity inherent in the design, which produces repeatable and quantifiable distortions, seismometers sometimes show other less predictable nonlinear effects, for example long-period transients after high-frequency seismic arrivals with a recorded amplitude that is well within the operating range of the sensor. They have been studied by, among others, Zahradník and Plešinger (2005, 2010), and Delorey *et al.* (2008), and probably most network operators have occasionally seen them in low-pass filtered records. Such transients can, for the horizontal components, theoretically result from a local coseismic tilt even when the sensor is perfectly linear. There is, however, often evidence that the transients are artifacts—for example when they seem to indicate a step in the vertical velocity or when sensors on the

same pier show completely different signals (J. M. Steim, personal comm., 2008; Zahradník and Plešinger, 2010). Possible explanations include ordinary nonlinearity, electronic clipping at frequencies outside the passband of the record, excitation of parasitic resonances causing nonlinearity, and thermal side effects of signal-dependent power consumption. It is also very likely that sudden onsets of seismic shaking can release pre-existing mechanical stresses in the suspension, or cause loosely connected parts (such as sensor feet on the pier, or a mass-centering device) to settle at a different position. Such phenomena occur spontaneously in newly manufactured or installed seismometers and it would be strange if they would not occasionally be triggered by seismic signals. In a two-tone test where one waits for the signal to become steady, they will hardly be noticed.

Conclusions

We have shown that nonlinear distortion in modern broadband seismometers can be measured on a vertical shake table that was not especially designed for this purpose. By exciting the table with two-tone signals at test frequencies from 0.25 to 8 Hz and a peak amplitude of 6.3 mm/s, we found rather uniform distortion levels of the acceleration in four widely used instrument types: STS1, STS2, CMG3-T, and Trillium 240. Low-frequency intermodulation was, on average, 96 dB below the test signal. Such a simple summary statement is only possible when all signals are expressed as equivalent ground accelerations. Distortion in terms of ground velocity or output voltage is larger and strongly dependent on the test frequencies. Distortion measured by injecting a two-tone signal into the calibration coil is obviously unrelated to the distortion of seismic signals, and in an STS2 gives a distortion ratio that is too optimistic by a factor of 30.

Data and Resources

All of the data presented in this research were collected at the Institute of Geophysics and Planetary Physics basement laboratory during the actual shake-table experiments, except those in the Appendix, which are from a control experiment at the Black Forest Observatory with entirely different hardware. The CALEX filtering software was searched using www.software-for-seismometry.de (last accessed February 2013).

Acknowledgments

We are indebted to many people at IGPP, including David Chavez, Peter Davis, Todd Johnson, and Glenn Sasagawa, who helped with these experiments by making seismometers available, configuring the data acquisition system, and maintaining the shake table. We thank reviewers for thoughtful and constructive suggestions. Funding for this experiment was provided by the National Science Foundation under Grant Number EAR0732418 and by the C. H. and I. M. Green Foundation for Earth Sciences.

References

- Delorey, A. A., J. Vidale, J. Steim, and P. Bodin (2008). Broadband sensor nonlinearity during moderate shaking, *Bull. Seismol. Soc. Am.* **98**, 1595–1601.
- Hutt, C. R., J. R. Evans, F. Followill, R. L. Nigbor, and E. Wielandt (2009). Guidelines for Standardized Testing of Broadband Seismometers and Accelerometers, *U.S. Geol. Survey Open-File Rept. 2009-1285*.
- Peterson, J., C. R. Hutt, and L. G. Holcomb (1980). Test and calibration of the seismic research observatory. *U.S. Geol. Survey Open-File Rept. 80-187*.
- Schuessler, H. W. (1981). A signal processing approach to simulation, *Frequenz* **35**, 174–184.
- Valliant, H. D., C. Gagnon, and J. F. Halpenny (1986). An inherently linear electrostatic feedback method for gravity meters, *J. Geophys. Res.* **91**, no. B10, 10463–10469.
- Wielandt, E. (2012). Chapter 5, Seismic sensors and their calibration, in *New Manual of Seismological Observatory Practice (NMSOP-2)*, P. Bormann (Editor), International Association of Seismology and Physics of the Earth's Interior, GFZ German Research Centre for Geosciences, Potsdam, <http://nmsop.gfz-potsdam.de/>.
- Zahradník, J., and A. Plešinger (2005). Long-period pulses in broadband records of near earthquakes, *Bull. Seismol. Soc. Am.* **95**, 1928–1939.
- Zahradník, J., and A. Plešinger (2010). Toward understanding subtle instrumentation effects associated with weak seismic events in the near field, *Bull. Seismol. Soc. Am.* **100**, 59–73.
- Zumberge, M., J. Berger, J. Otero, and E. Wielandt (2010). An optical seismometer without force feedback, *Bull. Seismol. Soc. Am.* **100**, 598–605.

Appendix

When Does Low-Frequency Distortion Matter?

A general statement on what level of low-frequency distortion is acceptable in practice cannot be made because for many purposes (for example, seismic monitoring) a moderate distortion of the signal is irrelevant. Among the more critical seismological tasks are the determination of coseismic ground displacement and the observation of free oscillations of the Earth. Assume, for example, that a regional earthquake has, over a time interval of 10 seconds and at frequencies around 4 Hz, the same rms amplitude as our test signal. Let the seismometer have a quadratic nonlinearity with an acceleration distortion ratio of -80 dB. The rms ac-

celeration is then nearly 80 mm/s^2 and equation (2) predicts an amplitude of $11 \text{ } \mu\text{m/s}^2$ for the static term. It would cause a spurious offset of 0.5 mm in the displacement trace after 10 s, which may represent a significant error. Nonlinearity in a seismogram from a short-period seismometer has a far more dramatic effect because at periods longer than the free period of the instrument, triple integration is required for the reconstruction of permanent ground displacement.

No one will expect to record undisturbed free modes in the presence of an earthquake signal sweeping through half of the operating range, but even much smaller signals can disturb free-mode recording when their envelope has substantial energy in the free-mode band. For example, even a good broadband seismometer with -100 dB quadratic-distortion ratio as in Figure 6 would be disturbed by high-frequency noise at 5–10 Hz whose rms amplitude is 0.25% of the operating range. Such noise can cause a beat signal that has more energy in the free-mode band than minimum ground noise, and if the envelope of the noise has periodic components, false spectral lines can appear in the free-mode spectrum.

Higher-Order Distortion

A more general approach than assuming a purely quadratic nonlinearity is to describe the distortion by a polynomial in the instantaneous amplitude: $Z(t) = g[z(t) + \sum \varepsilon_n z(t)^n]$. It is instructive to see what additional terms emerge from higher powers of $z(t) = \cos \omega_1 t + \cos \omega_2 t$. Expanding $z(t) = (\cos \omega_1 t + \cos \omega_2 t)^n$ into monochromatic terms yields the frequencies listed in Table A1.

The amplitudes of all spurious signals with frequencies other than ω_1 and ω_2 are comparable. We illustrate this mathematical result with spectra obtained by a numerical Fourier transformation of synthetic and real data. The synthetic two-tone signal consists of two sinewaves with 0.25 and 0.27 Hz and a duration of 300 s as shown in Figure 2. Trace 1 in Figure A1 in the Appendix is the logarithmic amplitude spectrum of this signal. The following spectra, traces 2–5 in the same figure, were obtained after adding second- to fifth-order distortions with a peak amplitude of 1% of the

Table A1
Intermodulation Frequencies for Different Exponents, n

n	Low Frequency	$\approx 1 \times$ Frequency	$\approx 2 \times$ Frequency	$\approx 3 \times$ Frequency	$\approx 4 \times$ Frequency	$\approx 5 \times$ Frequency
1		ω_1, ω_2				
2	$0, \omega_1 - \omega_2$		$2\omega_1, \omega_1 + \omega_2, 2\omega_2$			
3		$2\omega_1 - \omega_2, \omega_1, \omega_2, 2\omega_2 - \omega_1$		$3\omega_1, 2\omega_1 + \omega_2, \omega_1 + 2\omega_2, 3\omega_2$		
4	$0, \omega_1 - \omega_2, 2\omega_1 - 2\omega_2$		$3\omega_1 - \omega_2, 2\omega_1, \omega_1 + \omega_2, 2\omega_2, 3\omega_2 - \omega_1$		$4\omega_1, 3\omega_1 + \omega_2, 2\omega_1 + 2\omega_2, \omega_1 + 3\omega_2, 4\omega_2$	
5		$3\omega_1 - 2\omega_2, 2\omega_1 - \omega_2, \omega_1, \omega_2, 2\omega_2 - \omega_1, 3\omega_2 - 2\omega_1$		$4\omega_1 - \omega_2, 3\omega_1, 2\omega_1 + \omega_2, \omega_1 + 2\omega_2, 3\omega_2, 4\omega_2 - \omega_1$		$5\omega_1, 4\omega_1 + \omega_2, 3\omega_1 + 2\omega_2, 2\omega_1 + 3\omega_2, \omega_1 + 4\omega_2, 5\omega_2$

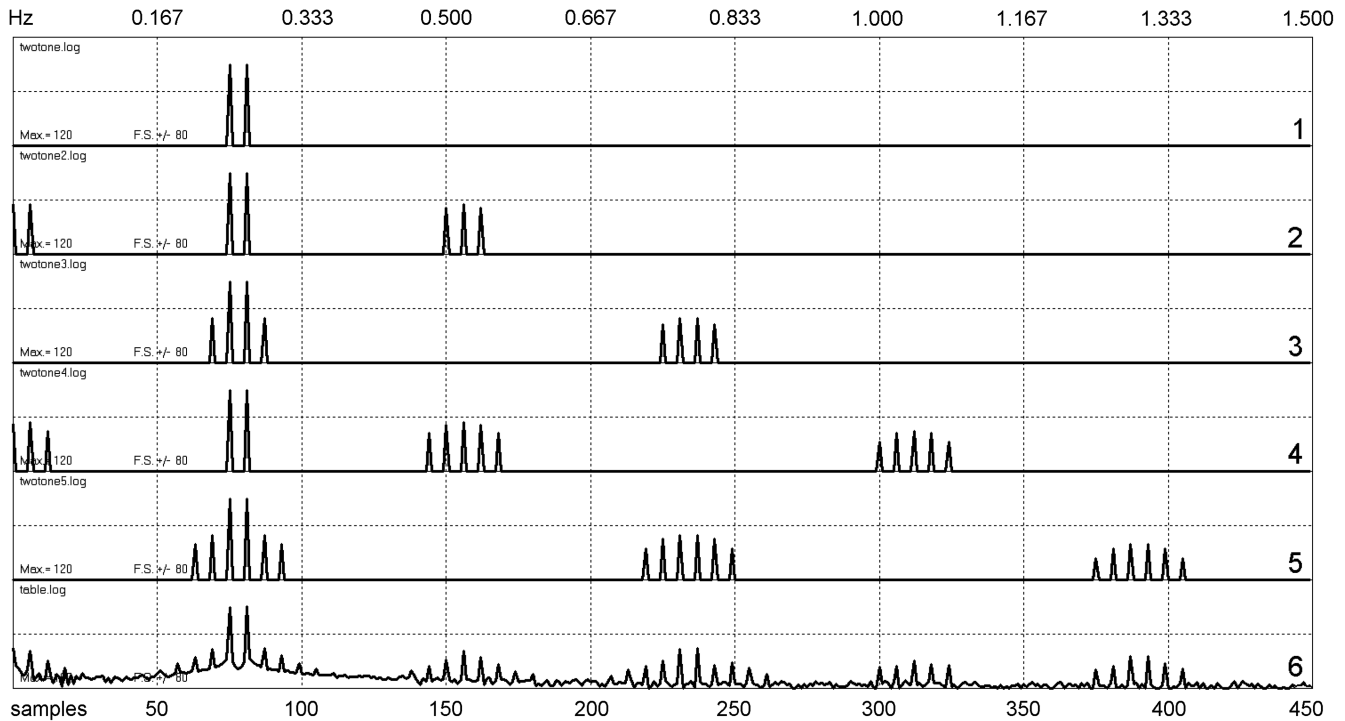


Figure A1. Logarithmic amplitude spectra of undistorted (1) and distorted synthetic test signals (2–5; the numbers correspond to the order of the nonlinear term). Full scale for each trace is 160 decibels. Only even-order nonlinearity causes low-frequency intermodulation. The last spectrum (6) is from the interferometrically measured displacement of the shake table. It shows low-frequency intermodulation of 68 dB below the rms displacement.

two-tone signal. Trace 6 shows distortion in the interferometrically measured displacement of the shake table. Evidently, at least for the shake table, a polynomial model predicts the spectral features of the distortion quite well.

Measuring Electrical Linearity

We have not systematically measured the electrical linearity of our seismometers because we consider it an irrelevant and misleading specification. Nevertheless, a few practical remarks and an example may be helpful. Measuring electrical linearity is an important test of the state-of-health of the seismometer electronics and is most useful if it can be done remotely, but electrical linearity does not guarantee overall linearity.

The measurement deserves some consideration because electrical distortion in the seismometer may be masked by distortion and noise from the signal generator and the digitizer, especially if one tries to record the calibration current via the voltage drop across a small resistor. We prefer to insert a solid-dielectric capacitor between the signal source and the coil (Figure A2 in the Appendix) and record the generator voltage across the capacitor and the coil. At seismic frequencies, the impedance of the circuit is dominated by the capacitor. Essentially, it determines the current as a time derivative

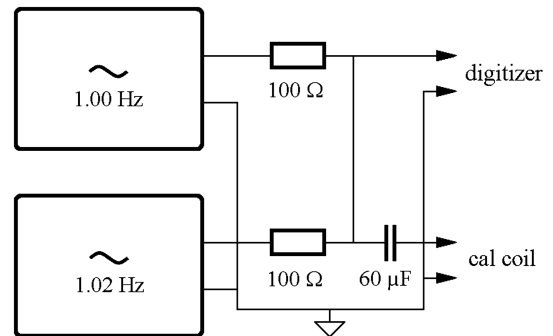


Figure A2. Suggested circuit for measuring the frequency response and the electrical distortion. Its purpose is explained in the text. The digitizer receives a signal that represents ground velocity while the calibration coil receives one that represents ground acceleration.

of the generator voltage. Because the current is equivalent to a ground acceleration, the generator voltage is nearly equivalent to a ground velocity. The output signal of a broadband-velocity seismometer then has nearly the same waveform as the generator signal and if the capacitance is well chosen, the signal even has nearly the same amplitude. Low-frequency distortions in both signals can be detected with the same resolution. This is convenient because the low-frequency distortion of the calibration current (the current through the capacitor) is by a factor (beat frequency/test frequency)

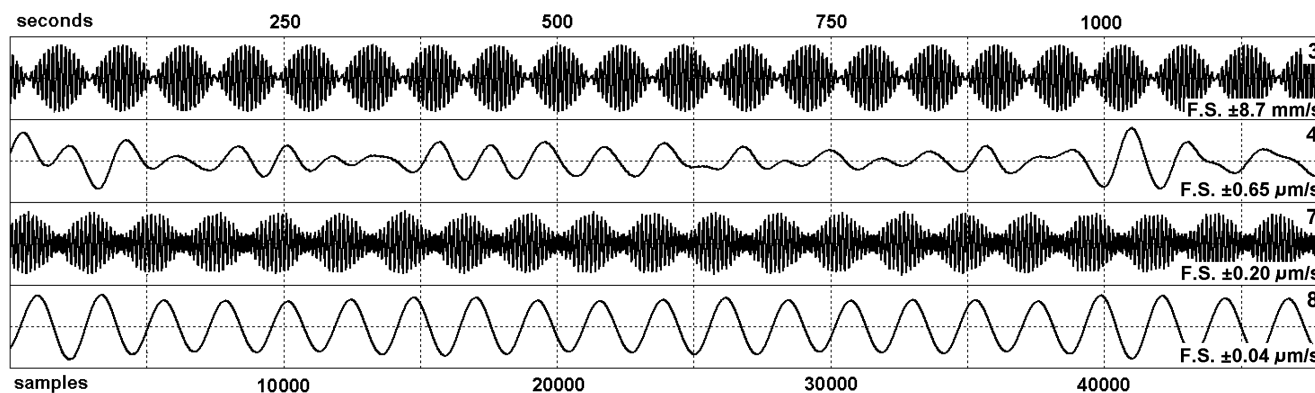


Figure A3. Seismometer output (3,4) and residual (7,8) from a test of electrical linearity. Traces are numbered as in Figure 4. Trace 8 (the filtered residual) is coherent with the envelope of the two-tone signal although it contains the signal of trace 4, which is much larger and less coherent.

smaller than that of the generator voltage and therefore difficult to observe directly.

The resistance of the calibration coil causes a small delay of the current, which can be included easily in the linear model. A theoretical disadvantage of this method is that it depends on the linearity of the coupling capacitor. We have, however, not encountered any problem with filter quality, solid-dielectric capacitors in this circuit. It is hard to imagine that such a capacitor would rectify a noticeable part of the alternating current flowing through it. A slight distortion of the current is certainly possible as the capacitance may depend on the applied voltage, but because even-order distortion would require a direct current to flow through the capacitor, this distortion must be of an odd order and cannot produce low-frequency intermodulation.

Digitizer nonlinearity may still interfere in a single experiment but can be identified and eliminated by repeating the experiment with polarity-reversed digitizer connections and evaluating the sum and the difference of the digital signals, which of course must be timed properly. Coupling two independent generators is preferable to using a single, amplitude-modulated generator. The signal from the latter can have a dc offset that would also be modulated, resulting in a much larger intermodulation signal than present in the combined signals of two independent generators running at constant amplitude. With a sweep, random-telegraph, or noise source in place of the two-tone source, the same setup and the same software (CALEX) serves to determine poles and zeros of the seismometer transfer function.

Figure A3 of the Appendix shows signals obtained with the circuit of Figure A2 of the Appendix. One of the

sinewave generators was a bit noisy, and some intermodulation also appears to be present in the generator signal (this was a control experiment with entirely different hardware). The method of evaluation is the same as described above, and the traces are numbered as in Figure 4. We have omitted traces 1, 2, 5, and 6 because they are visually identical to traces 3 and 4. Only the lowest test frequency of 0.25 Hz corresponding to the first wave group in Figure 4 is shown. The filtered output signal (trace 4) is dominated by noise from the generator. Because the same noise is present in the synthetic output signal, it cancels in the residual (trace 7), and we can clearly recognize the seismometer distortion in the filtered trace 8 at a level of -105 dB (velocity), -128 dB (acceleration), about 20 dB below generator noise. Obviously we are not even near the limit of resolution.

Institute of Geophysics
Stuttgart University
Azenbergstr. 16
70174 Stuttgart, Germany
e.wielandt@t-online.de
(E.W.)

Institute of Geophysics and Planetary Physics
Scripps Institution of Oceanography
University of California, San Diego
La Jolla, California 92093-0225
zumberge@ucsd.edu
(M.Z.)